REPUBLIK INDONESIA
KEMENTERIAN HUKUM

SURAT PENCATATAN CIPTAAN

Dalam rangka pelindungan ciptaan di bidang ilmu pengetahuan, seni dan sastra berdasarkan Undang-Undang Nomor 28 Tahun 2014 tentang Hak Cipta, dengan ini menerangkan:

Nomor dan tanggal permohonan	:	EC002025077546, 27 Juni 2025
Pencipta		
Nama	:	**Muhammad Zuhdi, S.Si.,M.T.**
Alamat	:	Perum Mapak Indah no 41, Sekarbela, Kota Mataram, Nusa Tenggara Barat, 82116
Kewarganegaraan	:	Indonesia
Pemegang Hak Cipta		
Nama	:	**Muhammad Zuhdi, S.Si.,M.T.**
Alamat	:	Perum Mapak Indah no 41, Sekarbela, Kota Mataram, Nusa Tenggara Barat, 82116
Kewarganegaraan	:	Indonesia
Jenis Ciptaan	:	**Karya Tulis Lainnya**
Judul Ciptaan	:	**Analysis of Gravity Gradients Tensor for Modeling The Earth's Crust Under Lombok Island**
Tanggal dan tempat diumumkan untuk pertama kali di wilayah Indonesia atau di luar wilayah Indonesia	:	27 Juni 2025, di Kota Mataram
Jangka waktu pelindungan	:	Berlaku selama hidup Pencipta dan terus berlangsung selama 70 (tujuh puluh) tahun setelah Pencipta meninggal dunia, terhitung mulai tanggal 1 Januari tahun berikutnya.
Nomor Pencatatan	:	000917807

adalah benar berdasarkan keterangan yang diberikan oleh Pemohon.
Surat Pencatatan Hak Cipta atau produk Hak terkait ini sesuai dengan Pasal 72 Undang-Undang Nomor 28 Tahun 2014 tentang Hak Cipta.

a.n. MENTERI HUKUM
DIREKTUR JENDERAL KEKAYAAN INTELEKTUAL
u.b
Direktur Hak Cipta dan Desain Industri

Agung Damarsasongko,SH.,MH.
NIP. 196912261994031001

Balai Besar Sertifikasi Elektronik

Disclaimer:
1. Dalam hal pemohon memberikan keterangan tidak sesuai dengan surat pernyataan, Menteri berwenang untuk mencabut surat pencatatan permohonan.
2. Surat Pencatatan ini telah disegel secara elektronik menggunakan segel elektronik yang ditertibkan oleh Balai Besar Sertifikasi Elektronik, Badan Siber dan Sandi Negara.
3. Surat Pencatatan ini dapat dibuktikan keasliannya dengan memindai kode QR pada dokumen ini dan informasi akan ditampilkan dalam browser.

Full Length Article

Analysis of Gravity Gradients Tensor for Modeling The Earth's Crust Under Lombok Island

Muhammad Zuhdi

[a] *Department of Physics, Faculty of Mathematics and Natural Sciences, Gadjah Mada University, Yogyakarta, 55000, Indonesia*

A R T I C L E I N F O

Keywords:
Lombok Island,
Gravity Gradient
Tensor, Earth
Crust, Modelling

A B S T R A C T

This study investigates the application of gravity gradient tensor (GGT) and total horizontal gradient (THG) methods to model the Earth's crust beneath Lombok Island, Indonesia, using satellite gravity data. Lombok is a geologically complex region located in a subduction zone, influenced by the interaction of the Indo-Australian, Eurasian, and Pacific plates. By utilizing satellite-based gravity measurements, this research aims to delineate vertical density boundaries and identify subsurface structures such as faults, intrusions, and uplifted zones. Forward modeling and inversion techniques were applied to gravity anomaly data, which were transformed into gravitational potential and subsequently into gradient tensors and horizontal gradients. The study demonstrates that THG provides clearer and more interpretable maps than GGT for identifying geological features. The resulting crustal density model offers valuable insights into the subsurface geology of Lombok Island and contributes to the understanding of tectonic activity in the region. This approach is expected to enhance geophysical exploration and hazard assessment, particularly in tectonically active and volcanically dynamic regions like Lombok. To the best of the authors' knowledge, this is the first implementation of GGT and THG satellite data analysis for crustal modeling in this region.

Keywords:
Gravity Gradient Tensor, Crustal Modeling, Lombok Island.

1. Introduction

Satellite gravity data is often chosen by earth researchers for various reasons including global coverage and availability of data in remote locations, high consistency and accuracy and availability of data over time. The advantage of using satellite gravity data is the availability of data throughout the earth's surface, even for areas that are difficult to reach. Satellites provide global coverage, which is important for mapping the Earth's gravity field as a whole, especially over oceans and remote areas that are difficult to access. (Tapley et al., 2004). Satellite data has other advantages, namely high consistency and accuracy. Satellite-based measurements are consistent and accurate over a long period of time. Satellite gravity data provide a high-precision model of the Earth's gravity field. (Wahr et al., 1998). Satellite gravity data are also available over time, allowing researchers to monitor dynamic changes in the gravity field. Satellite gravity data are invaluable for detecting and monitoring dynamic changes in the Earth's gravity field caused by geophysical processes such as plate tectonics, hydrological changes, and variations in ice mass. (Reigber et al., 2002).

Satellite gravity data enable us to conduct research on natural resources and subsurface structures. Local variations in the gravity field can provide important information about subsurface structures, including groundwater reserves, mineral deposits, and hydrocarbon resources. (Rummel et al., 2009). The use of satellite gravity data allows researchers to gain a better understanding of the Earth's gravity field, and the dynamics that influence it, in a more efficient and comprehensive manner.

The hypothesis of this study is that the Gravity Gradient Tensor and Total Horizontal Gradient of gravity are able to show vertical boundaries so that they can provide good analysis in modeling the density of the earth's crust. This study is limited to the use of the Gravity Gradient Tensor and Total Horizontal Gradient of gravity to show vertical boundaries so that they can provide good analysis in modeling the density of the earth's crust beneath the island of Lombok. This study is combined with inversion modeling of the density of the earth's crust with an initial model based on information obtained from the analysis of the Gravity Gradient Tensor and Total Horizontal Gradient. The gravity data used in this study is satellite gravity data. The assumption of this study is that the Gravity Gradient Tensor and Total Horizontal Gradient of gravity can show vertical boundaries of the earth's crust density model so that they can provide good analysis in modeling the density of the earth's crust by inversion beneath the island of Lombok. The objective of this study is to provide a density model of the earth's crust beneath Lombok Island by maximizing the analysis of the Gravity Gradient Tensor and the Total Horizontal Gradient.

The modeling of the earth's crust beneath Lombok Island based on the Gravity Gradient Tensor and the Total Horizontal Gradient of Gravity using satellite data, to the best of the author's knowledge, has never been done before. The analysis of the Gravity Gradient Tensor and the Total Horizontal Gradient of Gravity as the basis for the initial gravity inversion model is expected to be a novelty in this study.

2. Geology setting

Lombok Island is located in West Nusa Tenggara, Indonesia, with an area of about 4,725 km² and is part of the Lesser Sunda Islands. The island is bounded by the Lombok Strait to the west, which separates it from Bali, and the Alas Strait to the east, which separates it from Sumbawa. Lombok Island has volcanic mountains, the most famous of which is Mount Rinjani, the second highest volcano in Indonesia. Mount Rinjani, with a height of 3,726 meters, is one of the most active volcanoes in Indonesia and is the main geological feature on the island. (Hamilton, 1979). Mount Samalas on Rinjani volcanic complex explodes in 1257, wich is the greatest eruption along human history with estimated magnitude of 7 VEI (Lavigne, et al, 2013).

Lombok Island is located in a very complex zone tectonically. The tectonic setting of the island is influenced by the interaction between three major plates: the Indo-Australian Plate, the Eurasian Plate, and the Pacific Plate. Lombok is located in a subduction zone where the Indo-Australian Plate is diving beneath the Eurasian Plate, causing intense volcanic and seismic activity. (Katili, 1970). This island is part of the Sunda volcanic arc, which was formed by the subduction of the Indo-Australian Plate beneath the Eurasian Plate along the Sunda Trench. (Ben-Avraham and Emery, 1973). The volcanic activity in Lombok, especially around Mount Rinjani, is a direct result of this subduction process. Mount Rinjani has experienced several major eruptions, the most famous being the very powerful eruption of 1257. (Lavigne et al., 2013). In addition to the subduction zone, there is also strain tectonic activity behind the Sunda arc, which produces geological features such as cracks and collapses along the island. (Hall, 2012).

Lombok Island is an interesting area for geological study because of the complexity of its tectonic setting, its beautiful geomorphology, and its significant volcanic activity. Research continues to better understand the dynamics occurring in this area and their implications for geological hazards and natural resources. Lombok Island is an interesting area for geological study because of the complexity of its tectonic setting, its beautiful geomorphology, and its significant volcanic activity. Research continues to better understand the dynamics occurring in this area and their implications for geological hazards and natural resources.

Fault systems, intrusions and uplifted areas are widely found on Lombok Island, as shown in the geological map of Lombok (Suratno 1994, Mangga et.al, 1994). Generally, these fault systems are trending NE - SW and NW - SE (Katili 1989). The Lombok Fault (called the Lombok Fault: FL) is the longest fault, dividing Lombok Island into two parts, north and south (Figure 1). This fault extends from East to West. The most complex structure consisting of: faults, folds, intrusions and uplifted areas is found in South Lombok. The fault system is finger-like and related to various magmatic activities.

Several studies have been conducted related to faults on the island of Lombok and its surroundings using various geophysical methods. Stratigraphic mapping in the Java Sea (North Lombok) using the seismic reflection method (Astawa et al., 2005), mapping of Sembalun geothermal potential using gravity, geomagnetic and geoelectric methods (Herry 2007)

The gravity method can be used to detect faults, intrusions and uplifted areas in Lombok, as has been done by the following researchers. This gravity method has been successfully used for: i) Analysis and interpretation of subsurface structures (Coskun, 2006). ii) Studying the correlation between Bouguer anomalies and regional geology (Meurer and Ruess 2009). iii) Inversion of gravity anomalies in 2D and 3D interpretation of subsurface structures (Corehete et al. 2010, Richard et al., 2006). This research is very important, to analyze and model subsurface structures using gravity gradient tensor data. Conducting qualitative and quantitative interpretation of 2D inversion models of local subsurface geological structures.

The volcanoes around Lombok Island are located between 165 and 190 km above the Benioff zone, including Mount Rinjani, Tambora and Sangeang, all of which are still active (Bemmelen 1949). The structure of northern Lombok is a continuation of the Solo zone in Java, forming a mountain range (Darman and Saidi 2000). The loss of shallow and intermediate seismic activity in the Sunda Arc fault zone of South Lombok and Sumbawa has the potential for dangerous earthquakes. Defects and wrinkles in this area can cause deformation. Severe deformation in the eastern Lombok Basin is characterized by the presence of fault blocks, shale diapirs, and mud volcanoes (Hamilton 1979). As seen in Figure 1, faults are found in Selamat on the west of Mount Rinjani, Semberia and Pringabaya in East Lombok, and Sekotong in South Lombok.

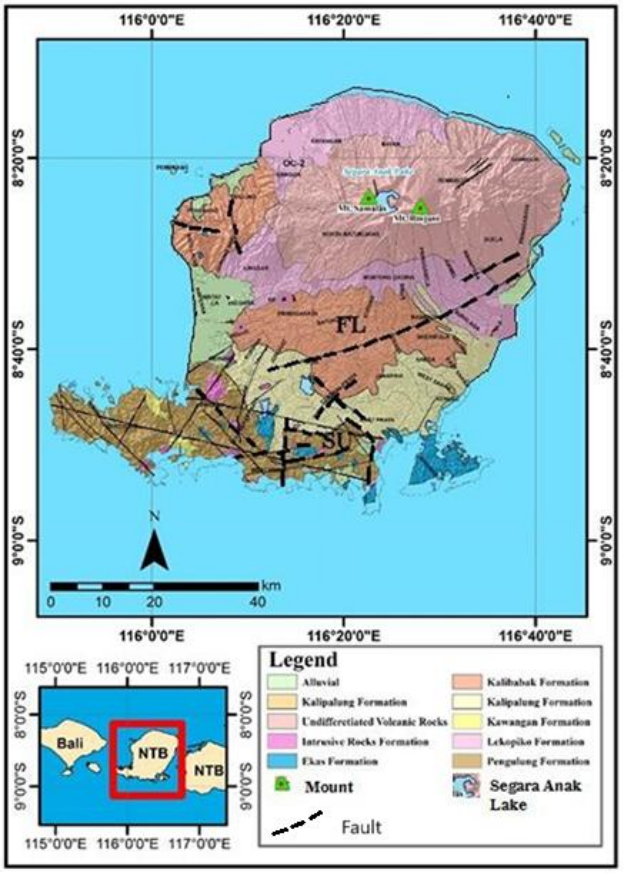

Fig. 1. Geology Map of Lombok Island (modified from Mangga 1994)

Middle Miocene magmatism is characterized by the emergence of a series of andesite and basalt intrusions that cut through the Penroll and Kawangan Formations. This intrusion caused the occurrence of sulfide mineralization and altered grains, as well as quartz veins, in the rocks of southern Lombok (Figure 1). These types of rocks and minerals have high density values.

The basic concept of subsurface density changes both laterally and vertically, which cause changes in the surface gravity field. The strength of the gravity field due to differences in buried mass (concentration or void space) is superimposed on the gravity field due to the total mass of the Earth. The two main components of the gravity field measured at the Earth's surface are, first, a general and relatively uniform component due to the total mass of the Earth; Second, a size component, the gravity anomaly, much smaller than the first component and varies, both laterally and vertically as the density changes. Estimation of gravity anomalies can be done using various techniques such as upward continuity.

Upward continuity is one method used to eliminate local or shallow anomalies and preserve local anomalies. Subtracting regional anomalies from global anomalies will produce local anomalies. To obtain a long-wavelength gravitational field wave field, in this case a local anomaly, observations can be made on another plane above the original observation plane (Blackely 1995). This only requires an inverse Fourier

transform. The basic principle of the upward continuation method is that when the observation point rises far above, the signal from the weak ground source will disappear. Therefore, what is obtained is the field generated by the main cause, namely the regional anomaly. The boundary conditions of the flat plane, where the source equivalent to the point mass has a depth of 2.5Δx <(h - zi) <6Δx (Dampney 1969). Where h is the depth of the point mass and zi is the average height of the topography, and Δx is the average distance between observation stations.

3. Methodology

3.1. Location and data collection

Satellite gravity data is often chosen by earth researchers for various reasons including global coverage and availability of data in remote locations, high consistency and accuracy and availability of data over time.

The advantage of using satellite gravity data is the availability of data throughout the earth's surface, even for areas that are difficult to reach. Satellites provide global coverage, which is important for mapping the Earth's gravity field as a whole, especially over oceans and remote areas that are difficult to access. (Tapley et al., 2004).

Satellite data has other advantages, namely high consistency and accuracy. Satellite-based measurements are consistent and accurate over a long period of time. Satellite gravity data provide a high-precision model of the Earth's gravity field. (Wahr et al., 1998).

Satellite gravity data are also available over time, allowing researchers to monitor dynamic changes in the gravity field. Satellite gravity data are invaluable for detecting and monitoring dynamic changes in the Earth's gravity field caused by geophysical processes such as plate tectonics, hydrological changes, and variations in ice mass.

Satellite gravity data enable us to conduct research on natural resources and subsurface structures. Local variations in the gravity field can provide important information about subsurface structures, including groundwater reserves, mineral deposits, and hydrocarbon resources. (Rummel et al., 2009).

The use of satellite gravity data allows researchers to gain a better understanding of the Earth's gravity field, and the dynamics that influence it, in a more efficient and comprehensive manner.

Earth gravity survey measurements using satellites are carried out by utilizing differences in gravitational fields at various locations on the earth's surface. The following are general steps in measuring earth gravity using satellites:

1. Introduction to Satellites: Satellites that are often used for gravity surveys are the GRACE (Gravity Recovery and Climate Experiment) satellite and the GOCE (Gravity field and steady-state Ocean Circulation Explorer) satellite. Both of these satellites are designed to measure changes in the earth's gravitational field with high precision.

2. Measuring Changes in Distance Between Satellites:
On the GRACE mission, there are two satellites orbiting the earth at a certain distance from each other. When they pass through areas with different gravitational variations, the distance between the two satellites will change.

The front satellite will be accelerated as it approaches an area with stronger gravity and the rear satellite will follow. Sensors on the satellites measure these changes in distance with high precision.

3. Gradiometer Measurement:
On the GOCE mission, the satellite is equipped with a gravity gradiometer that can measure the gravitational gradient. This instrument measures the acceleration experienced by the mass inside the satellite due to variations in the gravitational field.

This gradiometer provides data on changes in the gravitational field along the satellite's orbital path.

4. Data Collection and Processing:
Data collected by satellites are sent to ground stations for analysis. This data includes variations in the distance between satellites (for GRACE) or gravity gradients (for GOCE).

By processing this data, scientists can create more accurate and detailed models of the Earth's gravity field.

5. Applications of Gravity Data:
Gravity data from these satellites are used for various applications such as modeling ocean circulation, changes in ice mass, measuring sea level changes, and monitoring groundwater reserves.

Measurement of gravity data using satellites involves several steps and sophisticated technologies to obtain accurate information about the Earth's gravity field. Here is how it works and its mechanisms along with relevant quotes: Gravity satellites such as GRACE (Gravity Recovery and Climate Experiment) and GOCE (Gravity field and steady-state Ocean Circulation Explorer) use the principle of measuring changes in speed and distance between satellites to determine variations in the gravity field. (Tapley et al., 2004). GRACE consists of two identical satellites orbiting the Earth at a distance of about 220 kilometers. By measuring the changes in the distance between the two satellites with a high-precision microwave distance measuring system, variations in the Earth's gravitational field can be detected. (Wahr et al., 1998).

GOCE uses highly sensitive gradiometers to measure the gravity gradient along three axes. This allows for very precise measurements of the components of the gravitational field, thus providing detailed data on the Earth's gravitational anomalies. (Rummel et al., 2009).

The data obtained from these satellites are processed using sophisticated algorithms and models to correct for various factors, including atmospheric drag, ocean tides, and other forces, resulting in high-resolution gravity field maps. (Reigber et al., 2002).

With these advanced mechanisms and technologies, these satellites can provide gravity data with high resolution and accuracy, which is very useful for various geophysical studies and in-depth understanding of the internal structure and dynamics of the Earth.

Field is a physical quantity as a function of space and time which is a result of the existence of another physical quantity as its cause. The gravitational field is a physical quantity due to the physical quantity of mass as its cause. The earth's gravitational potential field U(x,y,z) is a scalar field, while the gravitational field strength g(x,y,z) is a vector quantity. The relationship between the gravitational potential field and the gravitational field strength is written as,

$$g_{(x,y,z)} = \nabla U_{(x,y,z)} \tag{3.1}$$

$$g_{(x,y,z)} = \frac{\partial U_{(x,y,z)}}{\partial x}\hat{\imath} + \frac{\partial U_{(x,y,z)}}{\partial y}\hat{\jmath} + \frac{\partial U_{(x,y,z)}}{\partial z}\hat{k} \tag{3.2}$$

$$g_{(x,y,z)} = g_{x(x,y,z)}\hat{\imath} + g_{y(x,y,z)}\hat{\jmath} + g_{z(x,y,z)}\hat{k} \tag{3.3}$$

The gravitational gradient which is the first derivative of the gravitational field strength with respect to position can be written as,

$$\nabla . g_{(x,y,z)} = \frac{\partial^2 U_{(x,y,z)}}{\partial x^2} + \frac{\partial^2 U_{(x,y,z)}}{\partial y^2} + \frac{\partial^2 U_{(x,y,z)}}{\partial z^2} \tag{3.4}$$

while the second derivative of the gravitational field strength can be written as,

$$\nabla^2 g_{(x,y,z)} = \frac{\partial^3 U_{(x,y,z)}}{\partial x^3}\hat{\imath} + \frac{\partial^3 U_{(x,y,z)}}{\partial y^3}\hat{\jmath} + \frac{\partial^3 U_{(x,y,z)}}{\partial z^3}\hat{k} \tag{3.5}$$

Equation (3.4) is often referred to as the first derivative of gravity or the gravitational gradient, while equation (3.5) is called the second derivative of gravity.

Gradient tensor and horizontal gradient of gravity

The gradient of gravity is the derivative of the value of the gravitational field strength with respect to position. The gravitational gradient is a tensor field that has 9 components. The horizontal gradient of gravity is part of the component of the gravitational gradient tensor field with the gradient direction to the x and y axes only against the value of the gravitational field in the z direction only.

The gravitational gradient tensor field is the result of a dyadic product between the nabla operator (∇) consisting of three components against the value of the gravitational field strength which also consists of 3 components. The dyadic multiplication equation can be written as,

$$\nabla g = \begin{pmatrix} \frac{\partial}{\partial x} \\ \frac{\partial}{\partial y} \\ \frac{\partial}{\partial z} \end{pmatrix} (g_x \quad g_y \quad g_z) \tag{3.6}$$

Substitute equation (3.5) into equation (3.6) without writing the position function (x,y,z) and unit vector (i ˆ, j ˆ, k ˆ), then we get the equation,

$$\nabla g = \begin{pmatrix} \frac{\partial g_x}{\partial x} & \frac{\partial g_y}{\partial x} & \frac{\partial g_z}{\partial x} \\ \frac{\partial g_x}{\partial y} & \frac{\partial g_y}{\partial y} & \frac{\partial g_z}{\partial y} \\ \frac{\partial g_x}{\partial z} & \frac{\partial g_y}{\partial z} & \frac{\partial g_z}{\partial z} \end{pmatrix} \tag{3.7}$$

By substituting equation (3.6) into equation (3.7), the value of the gravity gradient can be written as,

$$\nabla g = \begin{pmatrix} \frac{\partial^2 U}{\partial x^2} & \frac{\partial^2 U}{\partial x \partial y} & \frac{\partial^2 U}{\partial x \partial z} \\ \frac{\partial^2 U}{\partial y \partial x} & \frac{\partial^2 U}{\partial y^2} & \frac{\partial^2 U}{\partial y \partial z} \\ \frac{\partial^2 U}{\partial z \partial x} & \frac{\partial^2 U}{\partial z \partial y} & \frac{\partial^2 U}{\partial z^2} \end{pmatrix} \tag{3.8}$$

In gravity survey, the value of the gravitational field after various corrections and reductions to a flat plane, is located only on a flat plane, namely the (x,y) plane. The value of the gravitational field strength also only has one component, namely gz. The horizontal gradient of gravity is part of the component of the gravitational gradient tensor field with the gradient direction only to the x and y axes against the value of the gravitational field with a component in the z direction only. The horizontal gradient equation can be written as,

$$\nabla g = \begin{pmatrix} \frac{\partial}{\partial x} \\ \frac{\partial}{\partial y} \end{pmatrix} (g_z) \tag{3.9}$$

so that the horizontal gradient equation becomes simpler and is written in matrix form as,

$$\nabla g = \left(\frac{\partial g_z}{\partial x} \quad \frac{\partial g_z}{\partial y}\right) \tag{3.10}$$

Figure 1. Schematic diagram showing the components of the gravity vector (Gx, Gy, and Gz), the gradient tensor (Gxx, Gxy, Gxz, Gyx, Gyy, Gyz, Gzx, Gzy, Gzz), and the inclination angle (hx, hy, hz, and hMHC). The symbols A, MHC, and THDR represent the analytical signal, the magnitude of the horizontal component, and the total horizontal derivative, respectively. (Oruc and Keskinsezer, 2008)

Approximation value of horizontal gravity gradient numerically

The horizontal gravity gradient can be approached discretely by subtracting each measurement point in a certain direction. The derivative towards the x-axis is obtained by subtracting the gravity value of the measurement result at point xn+1, namely gn+1 from the gravity value at point xn, namely gn, then divided by the distance xn+1 to xn. To obtain the derivative value towards the y-axis, it is obtained by subtracting the gravity value of the measurement result at point yn+1 from the gravity value at point yn, then in the same way divided by the distance yn+1 to yn. The derivative approximation value of the y-axis, which is (gn+1-gn)/(yn+1-yn), is shown by the red slope in Figure 3.3. In the same way, the derivative approximation value of the y-axis is (gm+1-gm)/(ym+1-ym).

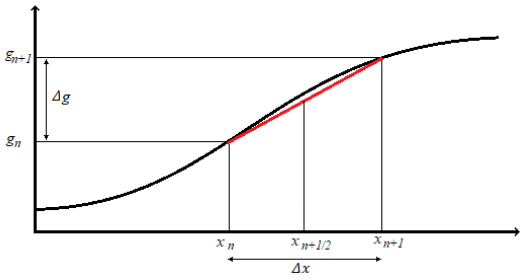

Figure 3.3 Horizontal derivative approach

In Figure 3.3, Δx is an approximation of the horizontal derivative value towards the x-axis at position n+1/2,m, so that Δx in the equation can be written as:

$$\frac{\Delta g x_{n+1/2,m}}{\Delta x} = \frac{g_{n+1,m} - g_{n,m}}{x_{n+1,m} - x_{n,m}} \tag{3.11}$$

In the same way, dy which is the horizontal derivative towards the y-axis at position n+1/2, m can be written as:

$$\frac{\Delta g y_{n,m+1/2}}{\Delta y} = \frac{g_{n,m+1} - g_{n,m}}{y_{n,m+1} - y_{n,m}} \tag{3.12}$$

The horizontal gradient value of gravity is the resultant vector derivative towards the x-axis with derivative in the y-axis direction. The horizontal gradient equation is then obtained by resulting with equations (3.10) and (3.11), so that we get,

$$\frac{\Delta g}{\Delta s} = \sqrt{\left(\frac{g_{n+1,m} - g_{n,m}}{x_{n+1,m} - x_{n,m}}\right)^2 + \left(\frac{g_{n,m+1} - g_{n,m}}{y_{n,m+1} - y_{n,m}}\right)^2} \tag{3.13}$$

4. Result and discussion

The gravity anomaly data is corrected for height to obtain the Bouguer anomaly. This Bouguer anomaly data is converted into gravity potential data considering that the gravity gradient tensor must be obtained from the potential field and not from the gravity field. This data is converted into gravity gradient tensor data and total horizontal gravity gradient data. From the gravity gradient tensor data, a gravity gradient tensor map (TGG) is obtained which consists of 9 components, namely Gxx, Gxy, Gxz, Gyx, Gyy, Gyz, Gzx, Gzy and Gzz, while from the total horizontal gradient data, a Single map is also obtained in the form of a total horizontal gravity gradient map. Interpretation is carried out from both types of maps.

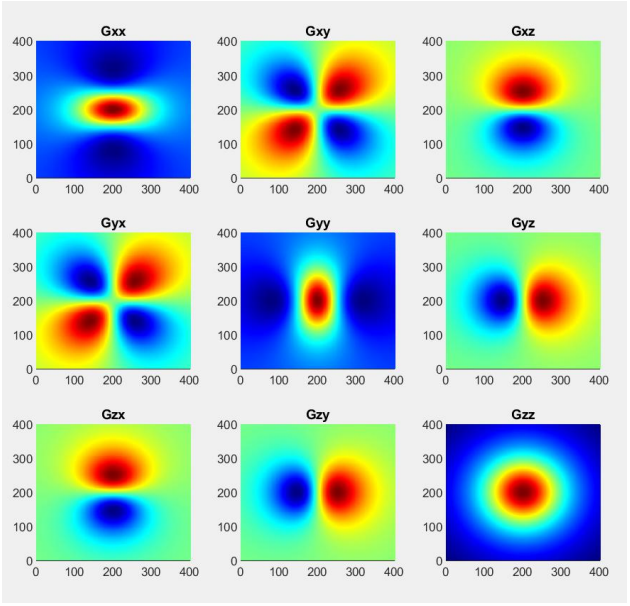

Figure 4.2 Gravity Gradient Tensor from the block model

Figure 4.2 shows the gravity potential field from the block-shaped anomalous object model. This forward modeling is carried out using Matlab with the convolution method to obtain the potential field from the block-shaped anomalous object. From the potential map of the modeling results, derivation is then carried out to obtain the gravity gradient tensor and the total horizontal gradient. Figure 4.4 shows a gravity gradient tensor map consisting of 9 components resulting from forward modeling of the subduction zone. Figure 4.5 shows a total horizontal gravity gradient map consisting of 9 components resulting from forward modeling of anomalous block-shaped objects.

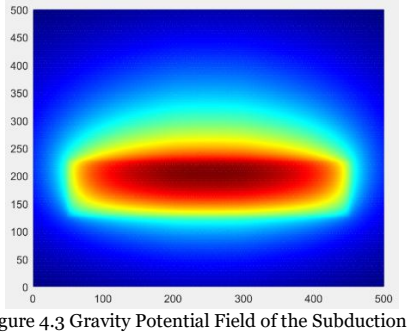

Figure 4.3 Gravity Potential Field of the Subduction Zone

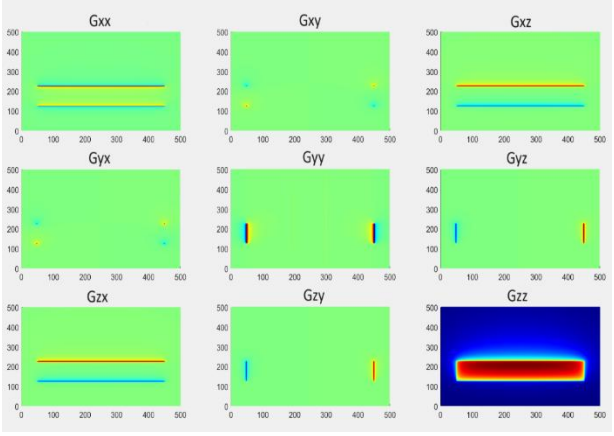

Figure 4.4 Gravity gradient tensor consisting of 9 components resulting from forward modeling of the subduction zone

Figure 4.3 shows the gravitational potential field of the subduction zone model. This forward modeling was performed using Matlab with the convolution method. From the potential map resulting from this modeling, derivation was then performed to obtain the gravity gradient tensor and the total horizontal gradient. Figure 4.4 shows a gravity gradient tensor map consisting of 9 components resulting from forward modeling of the subduction zone. Figure 4.5 shows a total horizontal gravity gradient map consisting of 9 components resulting from forward modeling of the subduction zone.

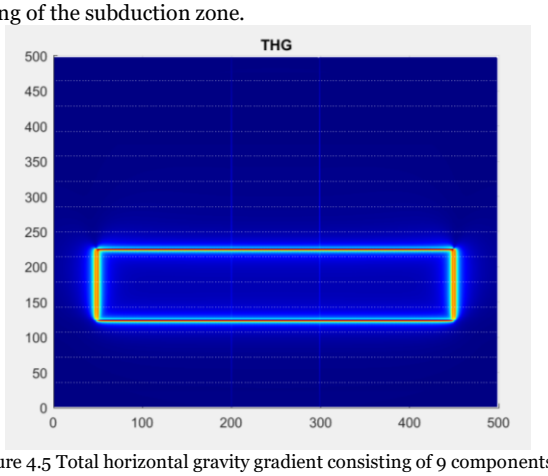

Figure 4.5 Total horizontal gravity gradient consisting of 9 components from forward modeling of subduction zones

Total Horizontal Gradient (THG) and Gravity Gradient Tensor (GGT) are two methods used in the interpretation of gravity data. Here are some reasons why THG can be considered to provide a better graphical representation compared to GGT: Simplicity of Visualization: THG produces simpler and easier to interpret maps, because it focuses on horizontal changes in the gravity field. This makes geological features such as faults or formation boundaries easier to recognize. Contrast Enhancement: THG tends to enhance the contrast between adjacent gravity anomalies, so that features that may not be visible in raw gravity data or in GGT become clearer. Linear Structure Detection: THG is very effective in detecting linear structures such as faults and faults, because this method is sensitive to lateral changes in the gravity field. Easier Data Processing: THG data processing and interpretation are often easier and faster compared to GGT, which requires more complex tensor analysis.

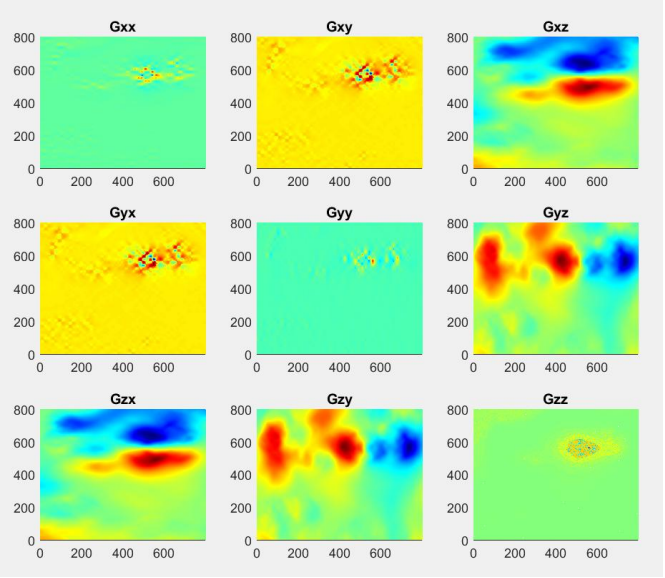

Figure 4.5 Gravity gradient tensor consisting of 9 components resulting from gravity satellite data of Lombok Island,

Author contribution

M.Z and W.S. developed research ideas for modelling earth crust under Lombok Island Nusa Tenggara Barat Province. W.A and S developed the concept and research design. M.Z collected and processed gravity data, drafted the journal manuscript. W.S and S proofread and

enrich and perfected the manuscript.

Data availability

Research data were obtained upon request and approval from all authors.

Declaration of competing interest

The authors declare that they have no known competing financial interests or personal relationships that could have appeared to influencethe work reported in this paper.

Acknowledgements

The author expresses gratitude to Curtin University for providing free high-resolution gravity field data from the GGMplus and SRTM2gravity models, as well as software for extraction and terrain correction. These resources significantly aided in data processing and allowed for efficient conclusions.

References

Abdelrahman, E.M., El-Araby, H.M., El-Araby, T.M., and Abbo-Ezz, E.R., 1993, Three least square minimization approaches to depth, shape, and amplitude coefficient determination from gravity data, Geophysics 66, 1105-1109.

Abdelrahman, E. M., El-Araby, H. M., El-Araby, T. M., and Abbo-Ezz, E. R., 2003, A least-squares derivatives analysis of gravity anomalies due to faulted thin slabs, Geophysics, Vol. 68, No. 2 (March-April 2003); P. 535–543, 11 Figs., 3 Tables.10.1190/1.1567222

Ansari, A.H. and Alamdar, K., A new edge detection method based on the analytic signal of tilt angle (ASTA) for magnetic and gravity anomalies, IJST (2011) A2: 81-88 Iranian Journal of Science & Technology.

Astawa, I.N, Ilahude D dan Kusnida D. 2005, Seismic Stratigraphy Sheet 1807 Water Lombok, West Nusa Tenggara, Journal of Marine Geology, vol. 3, no.3, (December) 8-14

Aydogan, D., 2011, Extraction of lineaments from gravity anomali maps using the gradien horizontal calculation: Application to Central Anatolia, Earth Planets Space, 63, 903–913, 2011

Bemmelen, R.W. van, The Geology of Indonesia. Martinus Nijhoff, The Huge, 1949.

Cai, L., Wan, X., Hsu, H., Ran, J., Meng, X., Luo, Z., & Zhou, Z., 2021, The earth's gravity feld recovery using the third invariant of the gravity gradient tensor from GOCE. Scientifc Reports (2021) 11:3581 https://doi.org/10.1038/s41598-021-81840-1

Chijun, Z., Shaofeng, B., Zhounm, Y., Lingtao, L. and Jian, F., 2011, Refining geoid and vertical gradien horizontal of gravity anomali, Geodesy and Geodynamics, 2(4):1 - 9http://www.jgg09.com Doi: lo.3724/SP.J. l246.2011.00009

Coskun, Sari and Mu¨jgan Salk, 2006, Sediment thicknesses of the western Anatolia graben structures determined by 2D and 3D analysis using gravity data, J. of Asian Earth Sciences, 26 39-48.

Corehete, V., Chourak, M., Khattach, D., 2010, A Methodolgy for Filtering and Inversion of Gravity Data, Engineering, 2, 149-159.

Darman, H. & Saidi, F.H., 2000, An outline of The Geology of Indonesia, IAGI.

Dampney, C.N.G., 1969, The Equivalent Source Technique, Geophysics v.34, no.1, p.39–35.

Djojoprajitno, A., 2000, Analisa Anomali Gravitasi 4D Daerah Panas Bumi Kamojang dengan Metode Korelasi, Thesis, Program Magister Teknik Geofisika Terapan ITB, Bandung

DUBEY, C.P., TIWARI, V. M.and. RAO, P. R, 2017, Insights into the Lurking Structures and Related Intraplate Earthquakes in the Region of Bay of Bengal Using Gravity and Full Gravity Gradient Tensor. Pure Appl. Geophys. 174, 2017, 4357–4368 Springer International Publishing AG DOI 10.1007/s00024-017-1661-4

Hall, R. 2012, Late Jurassic-Cenozoic reconstructions of the Indonesian region and the Indian Ocean. Tectonophysics, 570, 1-41. doi:[10.1016/j.tecto.2012.04.021](https://doi.org/10.1016/j.tecto.2012.04.021).

Hamilton, W., 1979, Tectonics of the Indonesia Region, Geological survey Professional paper 1078, Washington.

Katili, J.A., 1989, Geologi Indonesia, Majalah Ikatan Ahli Geologi Indonesia, Volume khusus 60 Thaun Prof. Dr. J.A Katili, vol.12, no.1, Juli

Katili, J. A., 1970, Large tectonic features of the Sunda Arc. Tectonophysics, 10(3), 237–260. doi:[10.1016/0040-1951(70)90021-0](https://doi.org/10.1016/0040-1951(70)90021-0).

Kusumoto, S., 2016, Dip distribution of Oita–Kumamoto Tectonic Line located in central Kyushu, Japan, estimated by eigenvectors of gravity gradient tensor., Earth, Planets and Space, 2016, 68:153 DOI: 10.1186/s40623-016-0529-7

Kusumoto, S., 2017, Eigenvector of gravity gradient tensor for estimating fault dips considering fault type. Progress in Earth and Planetary Science (2017) 4:15 DOI 10.1186/s40645-017-0130-0.

Lavigne, F., Degeai, J. P., Komorowski, J. C., Guillet, S., Robert, V., Lahitte, P., ... & Mangeney, A., 2013, Source of the great A.D. 1257 mystery eruption unveiled, Samalas volcano, Rinjani volcanic complex, Indonesia. Proceedings of the National Academy of Sciences, 110(42), 16742-16747. doi:[10.1073/pnas.1307520110](https://doi.org/10.1073/pnas.1307520110).

Mangga, S.A., Atmawinata, B. Hermanto, B. Setyonugroho and T.C. Amin, 1994, Geological Map Sheet Lombok, NTB, Geological research, and development center.

Matsumoto, N., Yoshihiro, H., Sawada, A., 2016, Continuity, segmentation and faulting type of active fault zones of the 2016 Kumamoto earthquake inferred from analyses of a gravity gradient tensor. Earth, Planets and Space, 2016, 68:167 DOI: 10.1186/s40623-016-0541-y

Oruc, B., 2010, Edge Detection and Depth Estimation Using a Tilt Angle Map from Gravity Gradien horizontal Data of the Kozaklı-Central Anatolia Region, Turkey, Pure Appl. Geophys. 2010 Springer Basel AG DOI 10.1007/s00024-010-0211-0

Oruc, B., and Keskinsezer, A., 2008, A Structural Setting of the Northeastern Biga Peninsula (Turkey) from Tilt Derivatives of Gravity Gradient Tensors and Magnitude of Horizontal Gravity Components, Pure appl. geophys. 165, 2008, 1913–1927 0033–4553/08/091913–15 DOI: 10.1007/s00024-008-0407-8

Pasteka, R., Zahorec, P., Kusnirak, D., Bosansky, M., Papco, J., Szalaiova, V., Krajnak, M., Marusiak, I., Mikuska, J., and Bielik, M., 2017, High resolution Slovak Bouguer gravity anomali map and its enhanced derivative transformations: new possibilities for interpretation of anomalous gravity fields, Contributions to Geophysics and Geodesy Vol. 47/2, 2017 (81–94)

Richard, A. Krahenduhl and Yaoguo Li, 2006 , Inversion of gravity data using a binary formation, Geophys, J.Int. 167, 543 – 556.

Reigber, C., Schwintzer, P., & Lühr, H., 2002, The CHAMP geopotential mission. Bollettino di Geofisica Teorica ed Applicata, 43(3-4), 221-226.

Rummel, R., Beutler, G., & Drinkwater, M. R., 2009, GOCE: The Earth gravity field as seen by space. Springer Science & Business Media .1.

Suratno, N, 1994, Maps Geology and Minerals Potential West Nusa Tenggara, Office of the Ministry of Mines and Energy NTB.

Tapley, B. D., Bettadpur, S., Watkins, M., & Reigber, C., 2004, The Gravity Recovery and Climate Experiment: Mission overview and early results. Geophysical Research Letters, 31(9), L09607. doi:[10.1029/2004GL019920](https://doi.org/10.1029/2004GL019920).

Tatchum, C.N., Tabod, T. C., Koumetio, F., and Manguelle-Dicoum, E., 2011, A Gravity Model Study for Differentiating Vertical and Dipping Geological Contacts with Application to a Bouguer Gravity Anomali Over the Foumban Shear Zone, Cameroon, Geophysica, 2011, 47(1–2), 43–55.

Telford, W.M., Geldart, L.P., Sherif, R.E., and Keys, D.A., 1990, Applied Geophysics, CambridgeUninversity Press, Cambridge.

Wahr, J., Molenaar, M., & Bryan, F., 1998, Time variability of the Earth's gravity field: Hydrological and oceanic effects and their possible detection using GRACE. Journal of Geophysical Research: Solid Earth, 103(B12), 30205-30229. doi:[10.1029/98JB02844](https://doi.org/10.1029/98JB02844).

Wahyudi. E. J., Kynantoro, Y., and Alawiyah, S., 2016, Second Vertical Derivative Using 3-D Gravity Data for Fault Structure Interpretation, International Conference on Energy Sciences (ICES 2016) IOP Publishing IOP Conf. Series: Journal of Physics: Conf. Series 877 (2017) 012039 doi :10.1088/1742-6596/877/1/012039.

Yuan, Y., Da-Nian, H., Qing-Lu, Y., Mei-Xia, G., 2013, Noise fi ltering of full-gravity gradient tensor data, APPLIED GEOPHYSICS, Vol.10, No.3 (September 2013), P. 241-250, 4 Figures. DOI: 10.1007/s11770-013-0391-3